4ICEGE
Thessaloniki-GREECE 2007

4th International Conference on
Earthquake Geotechnical Engineering
June 25-28, 2007
Paper No. 1529

THREE-DIMENSIONAL SHAKING TABLE TESTS ON SOIL-PILE-STRUCTURE MODELS USING E-DEFENSE FACILITY

Kohji TOKIMATSU[1] Hiroko SUZUKI[2], Kentaro TABATA[3], and Masayoshi SATO[4]

ABSTRACT

To investigate inertial and kinematic effects on failure and deformation mode of piles during three-dimensional shaking, physical model tests were conducted using the shaking table facility at the Hyogo Earthquake Engineering Research Center (E-Defense) of the National Research Institute for Earth Science and Disaster Prevention (NIED). A 3x3 steel pile group supporting a foundation with or without a superstructure was set in a dry sand deposit prepared in a cylindrical laminar box with a height of 6.5 m and a radius of 8.0 m. Experimental variables included the natural period of the superstructure and the presence of foundation. About 900 sensors were installed in the test models. The tests were conducted under one-, two- or three-dimensional shaking with three types of ground motion having a peak acceleration adjusted from 0.3 m/s^2 to 8.0 m/s^2. The piles yielded and buckled not only at their heads but also at depths from 0.7 m to 1.2 m during the final stage of shaking with peak input accelerations of 6.0 m/s^2 and 8.0 m/s^2, respectively, resulting in northeastward permanent deformation of piles as well as the inclination of the superstructure. The direction of pile deformation corresponds to those of the strong axes of ground displacement and acceleration, indicating that the ground displacement as well as inertial force had a significant effect on the failure of piles.

Keywords: Pile foundation, Soil-structure interaction, Large shaking table test, Failure mode

INTRODUCTION

To establish reliable seismic design of pile foundations, it is important to clarify the effects of inertia and kinematic forces on stress and failure of piles under actual earthquake loading conditions. Because of lack of well-documented case histories, physical model tests on pile foundations have been made based on 1-g and centrifugal shaking table studies. Most of those studies, however, concentrated on the effects of one-dimensional loading and rarely looked upon the effects of multi-dimensional shaking. Saito et al. (2002) conducted a soil-pile-structure interaction study using three-dimensional ground motions caused by mine blasting. The shaking induced by mine blasting was, however, insufficient to cause complete failure of pile foundation as well as to estimate inertial and kinematic effects on deformation and failure mode of piles in detail.

[1] Visiting Researcher, National Institute of Earth Science and Disaster Prevention, Professor, Department of Architecture and Building Engineering, Tokyo Institute of Technology, Japan, kohji@o.cc.titech.ac.jp
[2] Research Associate, Department of Architecture and Building Engineering, Tokyo Institute of Technology, Japan, hsuzuki@arch.titech.ac.jp
[3] Researcher, Hyogo Earthquake Engineering Research Center, National Institute of Earth Science and Disaster Prevention, Japan, tabata@bosai.go.jp
[4] Principal Senior Researcher, Disaster Prevention System Research Center, National Institute of Earth Science and Disaster Prevention, Japan, m.sato@bosai.go.jp

To investigate inertial and kinematic effects on failure and deformation mode of piles during three-dimensional shaking, physical tests on soil-pile-structure models were conducted (Tabata and Sato, 2006) using the shaking table at the Hyogo Earthquake Engineering Research Center (E-Defense) of the National Research Institute for Earth Science and Disaster Prevention (NIED). The E-Defense, one of the largest shaking table facilities in the world, was opened in 2005, commemorating the tenth anniversary of the 1995 Kobe earthquake. To investigate dynamic soil-pile-structure interaction and failure mechanism of pile foundation, a large cylindrical laminar box was constructed and two series of tests, one with a dry sand deposit and the other with a liquefiable saturated sand deposit, were conducted using the laminar box in the year of 2006. This paper describes the outline of the test using this facility as well as the deformation and failure mode of piles in the first test with a dry sand deposit made in the year of 2006.

SHAKING TABLE TESTS AT E-DEFENSE

Large shaking table tests with a soil-pile-structure model were conducted to investigate the following:

1) Inertial and kinematic effects on pile stress and failure.
2) Earth pressure acting on embedded foundation.
3) Stress states in soil and its effect on subgrade reaction development.
4) Deformation and failure mode of pile foundations under near prototype scale.

The E-Defense shaking table platform has a dimension of 15 m long and 20 m wide. It is supported on fourteen vertical hydraulic jacks and connected to ten horizontally hydraulic jacks, five each in both NS and EW directions, and can move in three-directions. It has a payload capacity of 1200 tons with maximum accelerations, velocities, and displacements of 9 m/s^2, 2m/s, and 1 m in both horizontal directions and of 15 m/s^2, 0.7 m/s, and 0.5 m in the vertical direction. About 900 channels of amplifiers and AD converters can be mounted under the shaking table platform for monitoring various outputs during shaking.

Fig. 1 and Photo 1 show a test model constructed in a cylindrical laminar box, 150 tons in total with a height of 6.5 m and a radius of 8.0 m, placed on the large shaking table. The cylindrical laminar box consists of forty-one ring flames, enabling shear deformation of the inside soil during

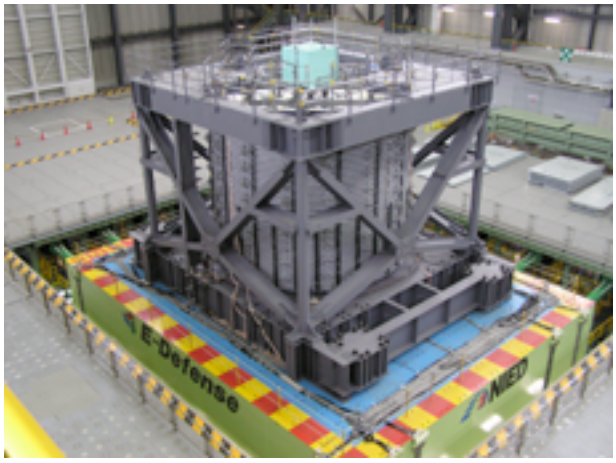

Photo 1 Test model on large shaking table

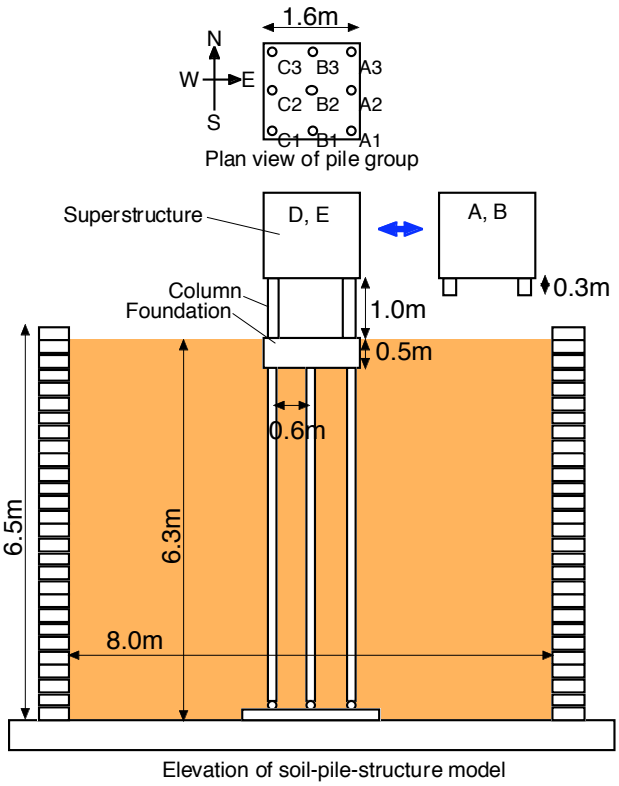

Fig. 1 Soil-pile-structure model

two-dimensional horizontal shaking. To minimize the occupation time of shaking table platform, the soil-pile-structure model was prepared at a preparation building located outside the shaking table building, carried by a lorry (Photo 2) into the shaking table building, and placed on the shaking table platform by two gigantic cranes. The total weight of the test model excluding the cylindrical laminar box and its attachments was 750 tons.

Albany sand was used for preparing the sand deposit. Fig. 2 shows the grain size distribution of the sand. The sand had a mean grain size D_{50} of 0.31 mm and a coefficient of uniformity U_c of 2.0. After setting the pile group in the laminar box, the sand was air-pluviated and compacted at every 0.275m to a relative density of about 70 % to form a uniform sand deposit with a thickness of 6.3 m.

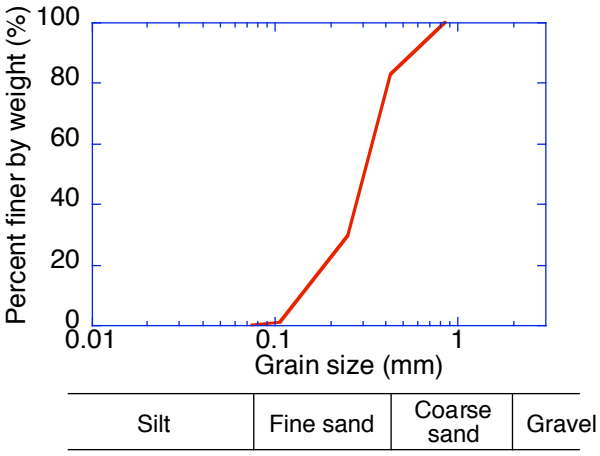

Fig. 2 Grain size distribution of Albany sand

Photo 2 Test model moved by lorry

Table 1 Test series

	Embedment	Superstructure	Natural period (s)	Maximum input acceleration (m/s^2)							
				JR Takatori				Taft and Tottori			
				X	Y	XY	XYZ	X	Y	XY	XYZ
A	Yes	Yes	0.1	0.3, 0.8				-			0.3, 0.8
B	Yes	Yes	0.6								
C	Yes	No	-								
D	Yes	Yes	0.2					0.3, 0.8			
E	No	Yes		0.3, 0.8			0.3, 0.8, 6.0, 8.0	-			

Table 2 Number of sensor channels

	Strain gauge	Accelerometer	Velocity meter	Earth pressure transducer	Displacement meter	Settlement meter	Load cell
Super-structure	0	12	4	0	7	0	0
Column	48	0	0	0	0	0	0
Foundation	0	12	0	16	4	0	0
Pile	476	28	0	52	0	0	27
Ground	0	63	0	0	2	5	0
Laminar box	0	82	0	0	24	0	0
Total	524	197	4	68	37	5	27

A 3x3 steel pile group was used for the test. The piles are labeled A1 to C3 according to their locations within the pile group, as shown in Fig. 1. Each pile had a diameter of 152.4 mm and a wall thickness of 2.0 mm. The piles were set up with a horizontal space of four-pile diameters center to center. Their tips were jointed to the laminar box base with pins and their heads were fixed to the foundation of a weight of 10 tons.

A total of five test series named A to E was conducted, in which the presence of foundation embedment and superstructure, and the natural period of the superstructure, as well as the type of input motions, and their components and maximum acceleration were varied. Table 1 shows the list of the test series. The foundation carried the superstructure of a weight of 28 tons in all series except for series C and had embedment except for series E. The superstructure had a natural period of 0.1, 0.2 or 0.6 s. This was achieved by changing the height and/or the rigidity of the four columns supporting the superstructure. The superstructure in series A was carried on steel columns 0.3 m high, that in series B on rubber columns 0.3 m high, and those in series D and E on steel columns 1.0 m high. The natural period of the ground is larger than that of the superstructure in series A, but smaller than that in series B, and closed to those in series D and E.

Table 2 shows the number of sensors used in the tests. Many strain gauges, accelerometers, velocity meters, earth pressure transducers, displacement transducers, settlement meters and load cells, about 900 sensors in total, were placed in the deposit as well as on the pile-structure model.

The tests were conducted under one-, two- or three-dimensional shaking with three types of ground motion, which were recorded at Takatori in the 1995 Kobe earthquake, at Lincoln School in the 1952 Taft earthquake and at Akasaki in the 2000 Tottori earthquake (hereby named Takatori, Taft, and Tottori). Figs. 3 and 4 show the time histories and acceleration response spectra of those motions. The acceleration response spectra were computed from acceleration records, on the assumption that a damping was 5 %. The acceleration response spectra of the horizontal motions at Tottori dominate only at a short period range with a sharp spectral peak at about 0.1 s (Fig. 4(c)), whereas those at Takatori and Taft dominate over a wide period range covering from 0.1 s to 1.0 s (Fig. 4(a)(b)). In each test series, either or both of the two horizontal or three-component motions

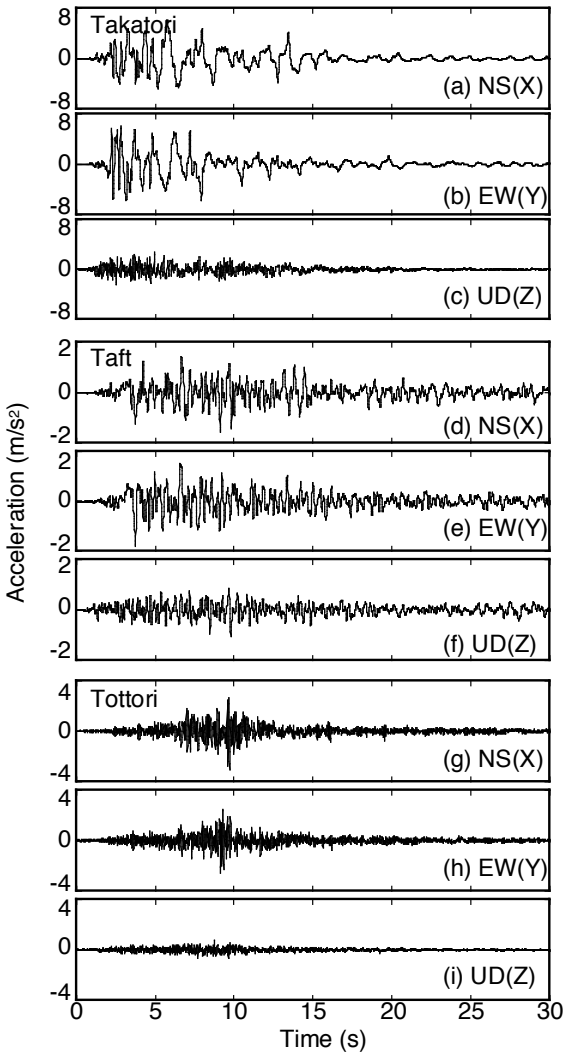

Fig. 3 Time histories of input motion

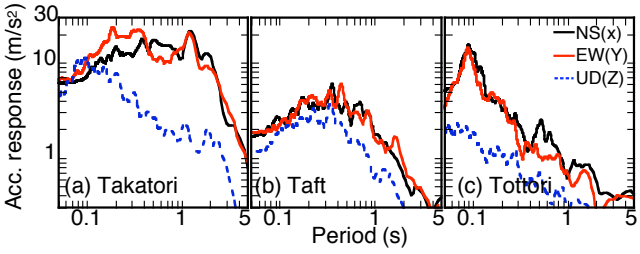

Fig. 4 Acceleration response spectra of input motion

were used as input shake table motions with the largest horizontal acceleration being scaled to a value listed in Table 1. The NS and EW components of the ground motion were applied to the NS (X) and EW (Y) directions as shown in Fig. 1, with the UD (Z) component to the vertical direction.

The test series were performed in alphabetical order, with increasing input shaking table acceleration in each test series. The strains induced in the piles were within the elastic range for any input motions with a maximum acceleration less than or equal to 0.8 m/s^2, keeping all the piles elastic until test series E. The piles, however, yielded at the pile heads as well as at 0.7 to 1.2 m below their heads and the superstructure inclined in test series E with input shake table accelerations of 6.0 m/s^2 and 8.0 m/s^2, respectively. This paper describes inertial and kinematic effects on deformation and failure mode of piles based on test series E with maximum input accelerations of 0.8 m/s^2 and 6.0 m/s^2.

DISTRIBUTION IN PILE STRESSES WITHIN PILE GROUP

Figs. 5 and 6 show the time histories of accelerations of superstructure, ground surface and shaking table in the NS, EW and UD directions and of bending strains of the NS and EW directions and axial strains at the heads of Piles A1, B2 and C3. The maximum acceleration of shaking table is

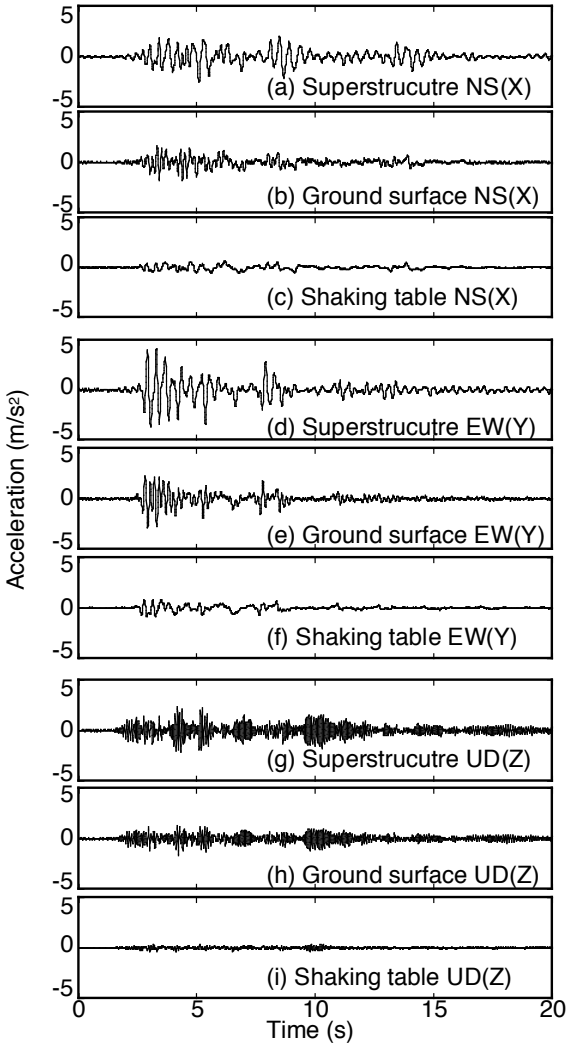

Fig. 5 Time histories of acceleration in test with input motion of 0.8 m/s^2

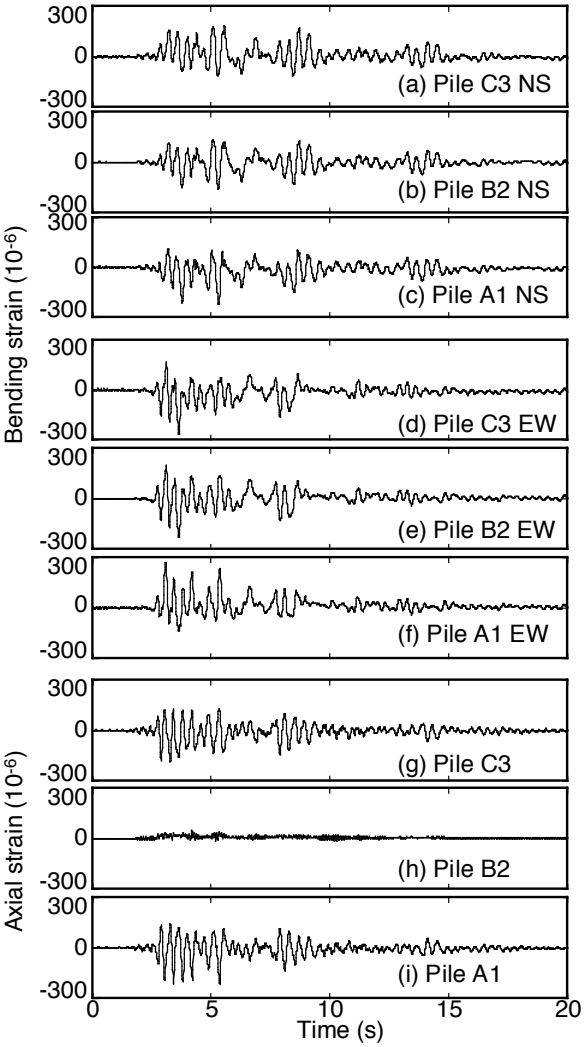

Fig. 6 Time histories of bending and axial strains in test with input motion of 0.8 m/s^2

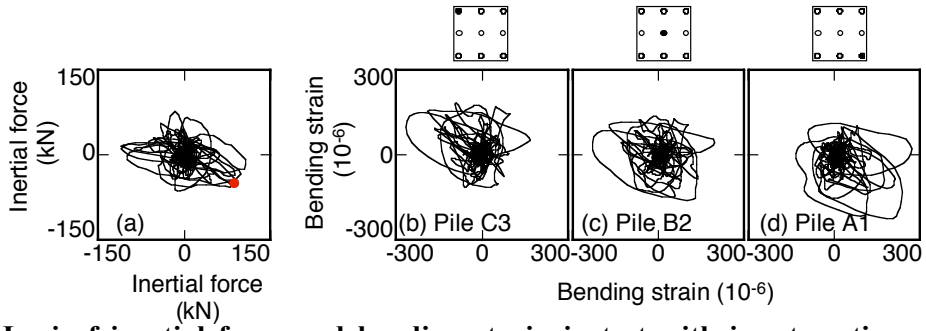

Fig. 7 Loci of inertial force and bending strain in test with input motion of 0.8m/s^2

0.8 m/s^2 in the horizontal directions and 0.4 m/s^2 in the vertical directions (Fig. 5(c)(f)(i)). The horizontal ground surface accelerations are more than twice as large as those of the shaking table (Fig. 5(b)(c)(e)(f)), and those of the superstructure are significantly larger than those of the ground surface (Fig. 5(a)(b)(d)(e)). The absolute axial strains in Piles A1 and C3 are almost the same with each other, but have opposite signals (Fig. 6(g)(i)). This is because Piles A1 and C3 are located on the opposite sides within a pile group and their axial forces due to overturning moment of the superstructure are reversed. The axial strain in Pile B2 is significantly smaller than those in Piles A1 and C3 (Fig. 6(g)(h)(i)), probably because Pile B2 is located in the center within the pile group. The bending strains of any pile tend to increase with increasing superstructure acceleration but show somewhat different trends depending on its location within the pile group. The bending strain in the EW direction is smaller on the negative side than on the positive side in Pile A1 but is smaller on the positive side than on the negative side in Pile C3 (Fig. 6(d)(f)). The bending strain in the NS direction, in contrast, is smaller on the positive side than on the positive side in Pile A1 but is smaller on the negative side than on the positive side in Pile C3 (Fig. 6(a)(c)). This suggests that the bending strain varies depending on the location within the pile group, as is the case in axial strain.

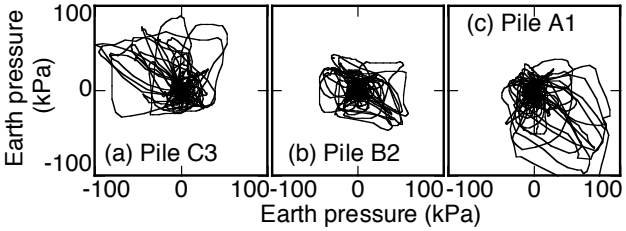

Fig. 8 Loci of earth pressure in test with input motion of 0.8 m/s^2

To investigate the variation of bending strain within the pile group, Fig. 7 shows loci of the inertial force of structure and bending strain in the horizontal plane. The inertial force was computed from the observed accelerations of superstructure and foundation. In Fig. 7, the horizontal axis indicates a component in the EW direction and the vertical one indicates a component in the NS direction. The inertial force is larger in the EW direction than in the NS direction and then its two-dimensional locus shows a spindle shape, the longer axis of which is in the EW direction (Fig. 7(a)). The loci of bending strain show the same trends as those of the inertial force. In addition, whenever the inertial force acts

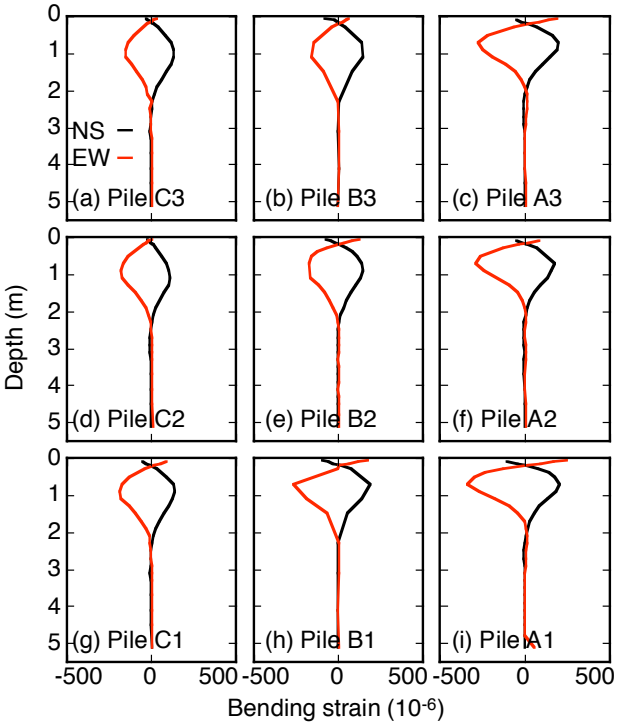

Fig. 9 Distribution of bending strain in test with input motion of 0.8 m/s^2

eastward, the bending strain becomes larger in Pile A1 than in Piles B2 and C3. In contrast, whenever the inertial force acts westward, the bending strain becomes larger in Pile C3 than in Piles A1 and B2. This indicates that the bending strain is the largest at the leading pile within the pile group.

Fig. 8 shows the loci of earth pressure near the ground surface in Piles A1, B2 and C3. The earth pressure in Pile A1 is larger on the southeast than any other direction and that in Pile C3 is larger on the northwest. The earth pressure in Pile B2, in contrast, does not show any directivity, keeping small values in any direction. The difference in earth pressure is probably caused by the group pile effects in which the stress zone induced by the following piles overlaps with those of the leading piles, causing a smaller earth pressure in the trailing piles than in the leading piles. The trends in earth pressures are consistent with those in bending strain, indicating that the group pile effect induces the difference in bending strain within the pile group.

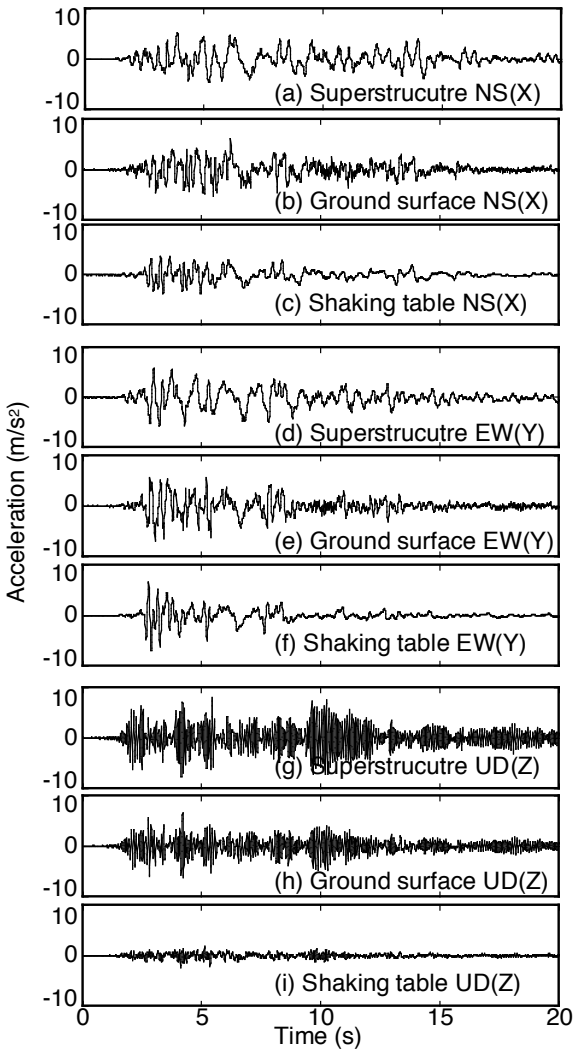

Fig. 10 Time histories of accelerations in test with input motion of 6.0 m/s^2

To estimate difference in bending strain within the pile group, Fig. 9 shows the distributions of bending strains in the NS and EW directions with depth for the nine piles when the inertial force takes the largest peak on the southeast, as shown by a circle in Fig. 7(a). At this moment, Pile A1 is the leading corner pile and Pile C3 is the trailing corner pile. Both NS and EW bending strains at the pile head as well as at a depth of about 1.0 m become the largest at the leading corner pile, i.e., Pile A1 (Fig. 9(i)), and become the smallest at the trailing corner pile, i.e., Pile C3 (Fig. 9(a)). In addition, the depth at which the bending strain takes the second largest peak tends to be shallower in the leading pile (Pile A1) (Fig. 9(i)) than in any other trailing pile, e.g., Pile C3 (Fig. 9(a)). These trends confirm that the pile stresses vary within the pile group and that bearing load is the largest in the leading corner pile.

INERTIAL AND KINEMATIC EFFECTS ON PILE DEFORMATION AND FAILURE MODE

Figs. 10 and 11 show the time histories of accelerations of the shaking table, ground surface and superstructure, as well as of bending and axial strains at the heads of the corner piles (Piles A1, A3, C1 and C3). The maximum shake table accelerations are 4.0 m/s^2 in the NS direction, 6.0 m/s^2 in the EW direction and 2.0 m/s^2 in the UD direction (Fig. 10(c)(f)(i)). The maximum horizontal acceleration of the superstructure is about 6.0m/s^2, which is closed to those of the shaking table and ground surface (Fig. 10(a)-(f)). This is different from the trends in the test with an input acceleration of 0.8 m/s^2, in which the horizontal accelerations of the superstructure are increased by a factor of 10 with respect to those of the ground surface and shaking table, being almost the same as those of the test with the input motions of 5.0 m/s^2. In spite of almost the

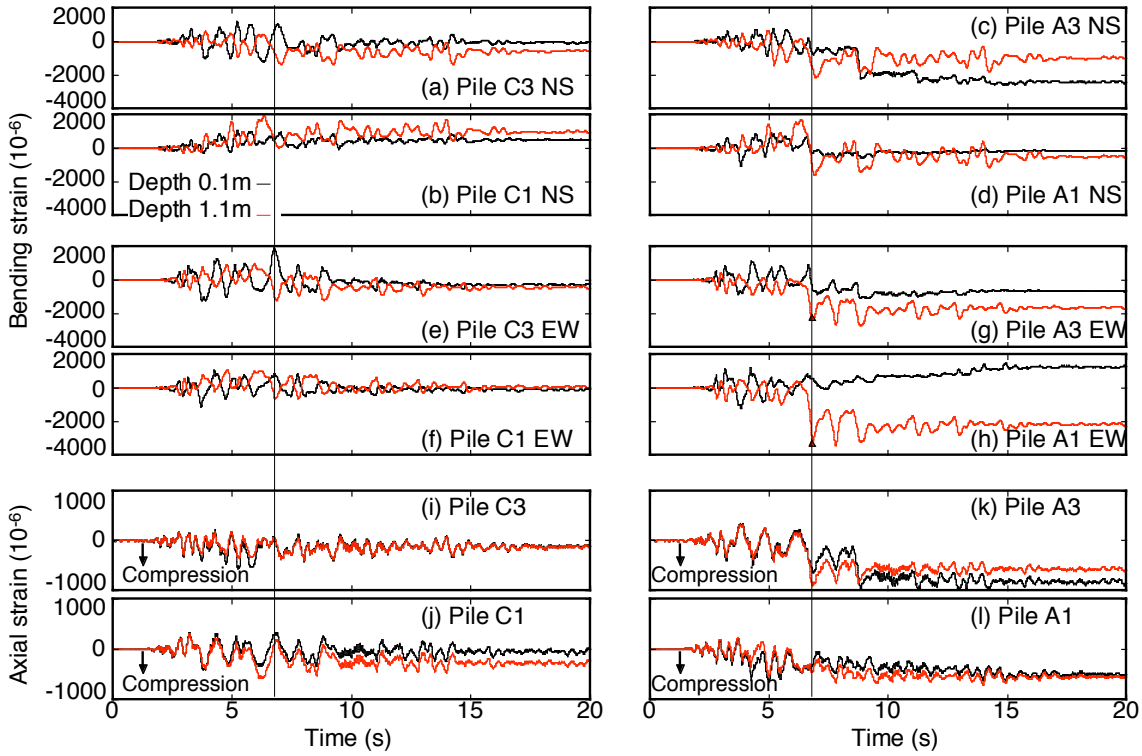

Fig. 11 Time histories of bending and axial strains in test with input motion of 6.0 m/s^2

same superstructure acceleration between the two tests, the bending strains are significantly larger at the later test with a greater input acceleration, showing residual values in some of the piles after about 6 s (Fig. 11(a)-(h)). This indicates that other factors rather than the inertial force might have affected the increase in bending strain. In addition, the axial strains have large residual values (Fig. 11(i)-(l)), particularly on the compression side in Pile A3 (Fig. 11(c)(g)(k)).

To investigate inertial and kinematic effects on deformation and failure mode of piles, Fig. 12 shows loci of inertial force, ground surface displacement and bending strain at pile heads in the horizontal plane. The locus of bending strain shows a similar trend to that of the ground surface displacement rather than that of the inertial force of the superstructure. The small circle in Fig. 12(a)(b) corresponds to the instance at which the bending strain in the leading corner pile takes the maximum for the duration of 1 s. Whenever the ground displacement increases, the bending strains increase, indicating that the kinematic effects arising from ground deformation have an important role on the increase in bending strain. The triangle in Figs. 11(g)(h)(k) and 12(a)(b) corresponds to the instance, about 6 s after the start of shaking, at which both bending and axial strains increase significantly, showing residual values in Pile A3 thereafter. Figures 11 and 12 indicate that, at this moment, both inertial force and ground displacement increase northeastward.

Fig. 13 shows the distributions with depth of bending strains of the nine piles at about 6 s after the start of shaking at which the piles start yielding. The figure shows that the bending strains at about 1 m depth in Piles A1, A2, and A3 exceed elastic limit and become closed to 3000 micro but that those in Pile C1 are within the elastic range. Because of the combined effects of inertial and kinematic forces acting on the same NE directions at about 6 s, the leading piles including Pile A3 bear larger forces than others and might have failed first.

After the test with a maximum acceleration of 6.0 m/s^2, a high input motion with a maximum acceleration of 8.0 was applied to the test model. The ground deformed significantly in the horizontal plane. The superstructure inclined toward northwest during the test. Photo 3 shows the inclined superstructure after the final test, compared with one before the test. Fig. 14 shows the residual deformation of the foundation, indicating that it not only moved northeastward but

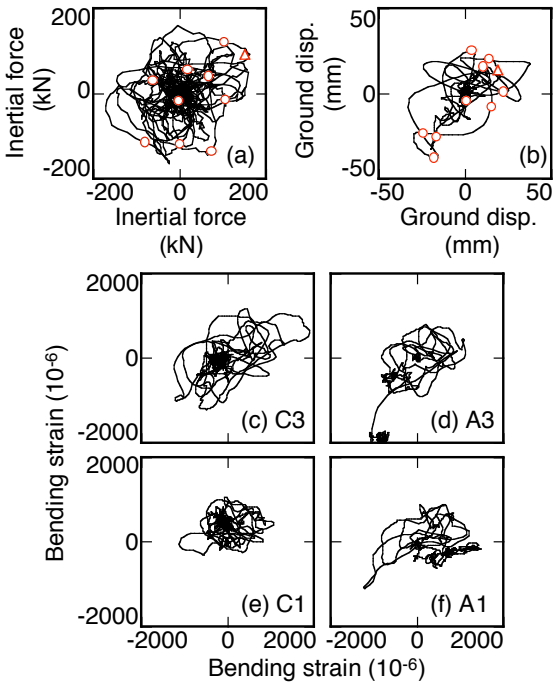

Fig. 12 Loci of inertial force, ground displacement and bending strain in test with input motion of 6.0 m/s^2

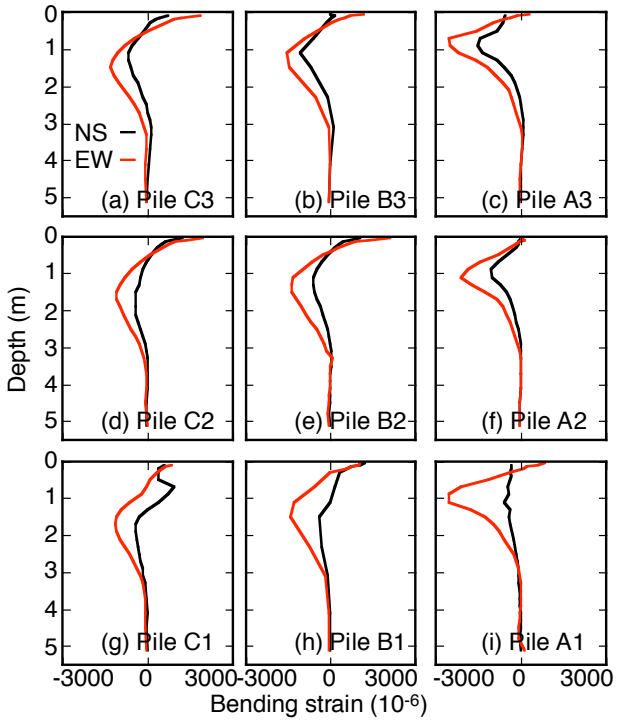

Fig. 13 Distribution of bending strain in test with input motion of 6.0 m/s^2

(a) Superstructure before test (b) Superstructure after test

Photo 3 Superstructure before and after tests

also rotated clockwise. Photo 4 shows the damage to pile foundations after excavation. Piles A1-A3 buckled at 1.2 m below their pile heads, the depth of which corresponds to the depth at which the measured bending strains take a peak in the ground (Fig. 13(c)(f)(i)). In contrast, Piles C1-C3 deform at 0.7 m below their pile heads, the depths of which do not correspond to the depths at which the measured bending strains take a peak at much deeper depths. This is probably because the damage firstly occurring in Piles A1-A3 led to redistribution of bearing load within the pile group.

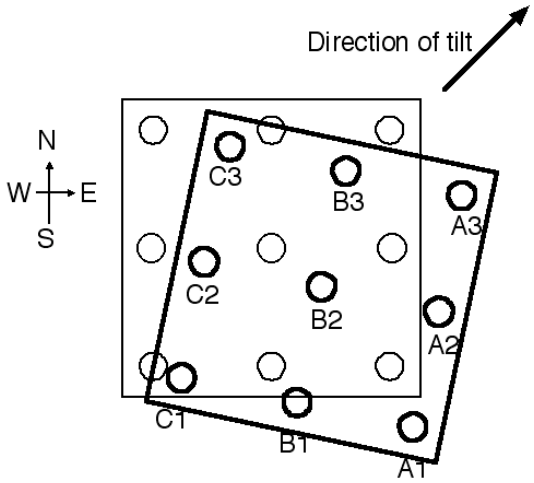

Fig. 14 Deformation of foundation after final test

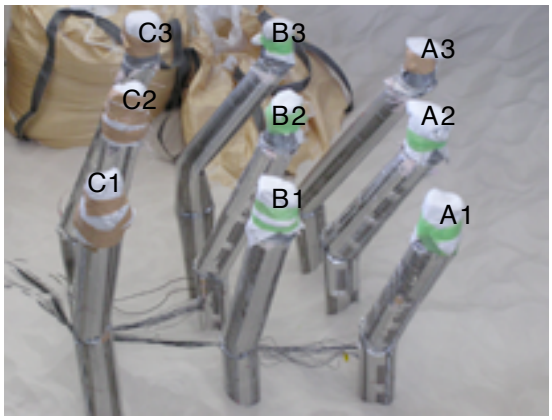

Photo 4 Damage to piles

CONCLUSIONS

To investigate inertial and kinematic effects on failure and deformation mode of piles, physical model tests on soil-pile-structure systems were conducted using the large shaking table at E-Defense, NIED. The test results and discussions have led the following:

1) The first dynamic soil-pile-structure interaction study using E-Defense shaking table and two-dimensional laminar box was successfully made with the piles severely damaged at the final stage of shaking. About 900 sensors installed in the test model were in good conditions throughout the tests and could provide valuable data for examining soil-pile-structure interaction effects and failure mechanism of pile foundation under three dimensional shaking.

2) The leading piles attract earth pressure more than the trailing piles, probably reflecting group pile effects. As a result, the bending strain is larger in the leading piles than in the trailing piles and the depth at which the inflection of bending strains occurs is shallower in the leading piles than in the trailing piles.

3) The piles yielded and the superstructure inclined under the input motion with a maximum acceleration of 6.0 m/s^2 and 8.0 m/s^2, respectively. The piles not only suffered local buckling at their heads but also deformed significantly at 0.7 m to 1.0 m below their heads.

4) The direction of permanent pile deformation corresponds to those of the strong axis of inertial force and ground displacement, indicating that the ground displacement as well as the inertial force could have significant effects on pile deformation and failure.

AKNOWLEDGEMENTS

The study described herein was made possible through Special Project for Earthquake Disaster Mitigation in Urban Areas, supported by the Ministry of Education, Culture, Sports, Science and Technology (MEXT). The authors express their sincere thanks to the above organization.

REFERENCES

Saito, H., Tanaka, H., Ishida, T., Koyamada, K., Kontani, O. and Miyamoto, Y., "Vibration tests of pile-supported superstructure in liquefiable sand using large-scale blast (Outline of vibration tests and responses of soil-pile-structure)", Journal of Structural and Construction Engineering, 553, 41-48, 2002 (in Japanese).

Tabata, K. and Sato, M., Report of special project for earthquake disaster mitigation in urban areas, Ministry of Education, Culture, Sports Science and Technology, 489-554, 2006 (in Japanese).